Surface Eu-Treated ZnO Nanowires with Efficient Red Emission

Rui Chen,[†] Y. Q. Shen,[‡] F. Xiao,[†] B. Liu,[†] G. G. Gurzadyan,[†] Z. L. Dong,[‡] X. W. Sun,[§] and H. D. Sun*,[†]

Division of Physics and Applied Physics, School of Physical and Mathematical Sciences, Nanyang Technological University, Singapore 637371, Singapore, Division of Materials Science, School of Materials Science and Engineering, Nanyang Technological University, Singapore 639798, Singapore, and Division of Microelectronics, School of Electrical and Electronic Engineering, Nanyang Technological University, Singapore 639798, Singapore

The structural and optical properties of post surface Eu-treated ZnO nanowires (NWs) have been investigated systematically. It is found that the Eu^{3+} ions are in the Eu_2O_3-like state located at the surface of ZnO NWs. Sharp intense red emissions in the range of 580−650 nm due to the intra-4*f* transition of Eu^{3+} ions are observed from the sample. The temperature-dependent photoluminescence (PL) measurement shows that the intensity of the Eu^{3+} ions emission is related to the near-band-edge (NBE) emission of ZnO NWs, indicating direct energy transfer from ZnO to Eu^{3+} ions. Finally, the time-resolved PL measurement was carried out, and the roles played by the Eu_2O_3-like layers are discussed in detail. It is found that the Eu_2O_3 layers not only suppress the deep level emission (DLE) in ZnO NWs but also provide efficient energy trap centers supporting the direct energy transfer from ZnO to Eu^{3+} ions.

Introduction

Wurtzite-type ZnO, a wide bandgap (3.37 eV) polar semiconductor with a large exciton binding energy (∼60 meV) at room temperature,[1] has been recognized as a promising material for ultraviolet (UV) light-emitting devices (LEDs) and laser diodes.[2,3] The emission wavelength of ZnO-based materials can be tuned by alloying with other elements, for example, Mg or Be for shorter wavelengths[4,5] and Cd for longer wavelengths.[6,7] For some particular applications such as full color flat panel display and solid-state lighting, three primary colors (red, green, and blue) are required. ZnCdO-based devices are suitable for blue−green light emitters; however, it is hard to achieve high efficient red emission because of the phase separation during material growth with high Cd concentrations.[8] On the other hand, rare-earth element doped wide bandgap semiconductors have become attractive for some selective wavelength emissions. The large bandgap of the host material allows higher efficiency device applications at room or even higher temperatures. This approach has been demonstrated successfully in Eu^{3+}-doped GaN material.[9] To harvest intense Eu^{3+} emission from ZnO, an efficient energy transfer from the host to Eu^{3+} ions is required. However, there have been very few reports on the synthesis and investigations of the optical properties of Eu-doped ZnO nanowires (NWs) with intense red emission.[10]

For the fabrication of Eu^{3+}-doped ZnO material, several kinds of methods such as pulse laser deposition (PLD),[11] hydrothermal,[10] and ion implantation techniques[12] have been employed. However, up until now, for red emission in Eu^{3+}-doped ZnO NWs, the Eu^{3+} ions were incorporated into the matrix during growth.[10,11,13−16] Motivated by the intensive interest in ZnO-based NWs LEDs,[17] we have studied the structural and optical

properties of post surface Eu-treated ZnO NWs. It is found that the sample exhibits intense red emission from the intra-4*f* transition of Eu^{3+} ions, which may provide a viable approach for efficient red light source for ZnO-based devices. The temperature-dependent photoluminescence (PL) measurement indicates direct energy transfer from ZnO to Eu^{3+} ions. The surface modification of the Eu_2O_3-like layer and the mechanism of energy transfer are discussed in detail.

Experimental Section

The ZnO NWs used herein were fabricated on a *c*-plane sapphire substrate by a vapor phase transport (VPT) method. ZnO (99.99%, Alfa Aesar) and graphite powder (99.99%, Aldrich) with a 1:1 weight ratio on the Sapphire substrate were precoated with a 20 nm Au film. The source was placed in the center of a horizontal tube furnace maintained at 950 °C. The europium acetate powders were dissolved in deionized water, and then urea was employed to tune the pH value (∼6.5) of the solution to exclude damage of ZnO. The as-grown ZnO NWs were then treated with the solution and followed by a thermal annealing at 500 °C in air for 3 h. Simultaneously, another pure ZnO NW sample was annealed under identical conditions for reference.

The crystal structure of the ZnO NWs was characterized by X-ray powder diffraction (XRD) using a Bruker D8 Advanced diffractometer and Cu Kα radiation. Morphological characterization was performed with a JEOL JSM-6700F field emission scanning electron microscope (FESEM) and a JEOL 2100 transmission electron microscope (TEM). The PL measurements were performed between 10 and 300 K by using a closed cycle helium cryostat. A cw He−Cd laser emitting at 325 nm was used as excitation source, and the signal was dispersed by a 750 mm monochromator combined with suitable filters and detected by a photomultiplier using the standard lock-in amplifier technique.[18] Time-resolved photoluminescence (TRPL) was carried out at room temperature by the time-correlated single

* To whom correspondence should be addressed. E-mail: hdsun@ntu.edu.sg.
[†] Division of Physics and Applied Physics.
[‡] Division of Materials Science.
[§] Division of Microelectronics.
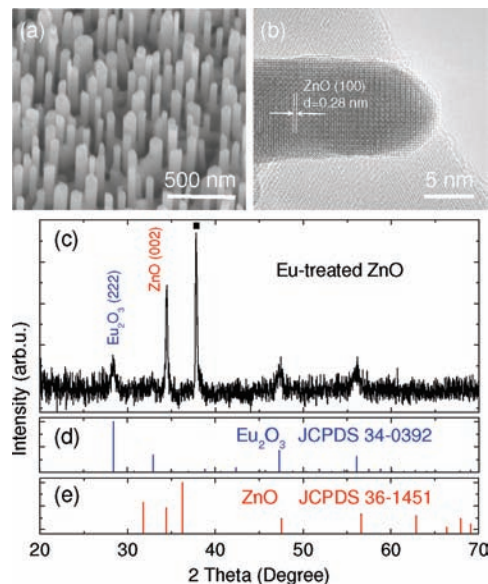
Figure 1. (a) FESEM image of the annealed ZnO NWs. (b) High-resolution TEM of the Eu-treated ZnO NWs. (c−d) The XRD pattern of Eu-treated ZnO NWs and the reference of pure Eu_2O_3 and ZnO. The peak denoted by a closed square is from sapphire substrate.

photon counting (TCSPC) technique, with a resolution of 10 ps (PicoQuant PicoHarp 300), and the 295 nm pulse laser (100 fs, 80 MHz) from the third harmonic of the Titanium sapphire laser (Chameleon, Coherent Inc.) was used as an excitation source.

Results and Discussion

As shown in Figure 1a, the annealed pure ZnO NWs are found vertically aligned on the substrate with a length of only 300−400 nm. A high-resolution TEM image (Figure 1b) reveals sharp and clear ordered-lattices in the center of the post Eu-treated ZnO NW. The interplanar *d*-spacing is 0.28 nm, which corresponds to the (100) plane of the hexagonal ZnO. In contrast, the outer-shell of the Eu-treated ZnO NW exhibits relatively oblique and disordered-lattices, which can be attributed to the presence of Eu_2O_3 on the surface.[19] Figure 1c−e shows the XRD patterns of Eu-treated ZnO NWs together with Eu_2O_3 and ZnO for comparison. The XRD patterns of the sample can be indexed as coming from Eu_2O_3 and ZnO. It is well-known that the radius of Eu^{3+} (0.95 Å) is bigger than Zn^{2+} (0.74 Å); thus, the diffraction peaks are expected to shift toward smaller angles if Eu^{3+} entered the Zn^{2+} lattice sites. However, no shifts in the XRD peaks for Eu-treated ZnO were observed. Therefore, the investigation suggests that almost all of the Eu^{3+} ions are in Eu_2O_3 oxide, which is just located at the surface of the ZnO NWs. This is also supported by the optical measurements performed later.

Figure 2 depicts the room temperature PL spectra of annealed ZnO NWs with and without Eu^{3+} treatment. The pure ZnO sample exhibits an emission band at 380 nm, which is attributed to the near-band-edge (NBE) emission. A strong green emission band located at ~515 nm is also observed, which is corresponded to oxygen vacancy (V_O) and denoted as deep level emission (DLE).[20] In comparison, it is interesting to note that the emission of Eu-treated ZnO NWs demonstrates a dramatic decrease in the green emission. It is well-known that the Eu^{2+} ions in crystal give a broad emission band in the same wavelength range due to the *f−d* transition.[13] However, here we used Eu^{3+} solution for treatment, and the presence of Eu^{2+}
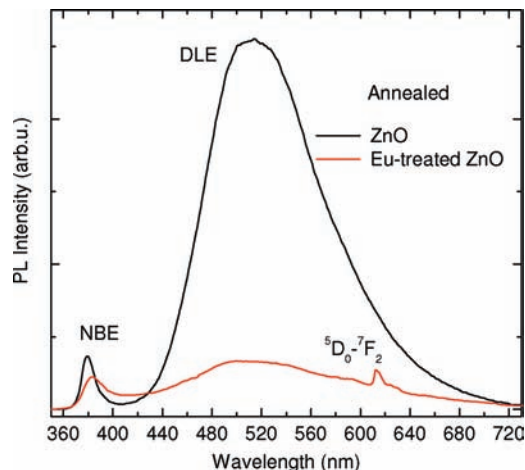

Figure 2. Room temperature PL spectra of the ZnO NWs with and without Eu^{3+} treatment.
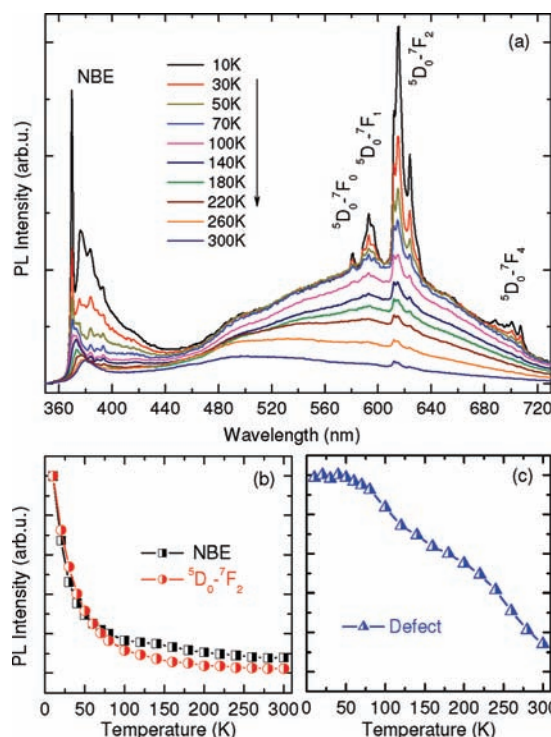
Figure 3. (a) Temperature-dependent PL spectra of Eu-treated ZnO NWs from 10 to 300 K. (b−c) The intensity of the NBE, the $^5D_0-^7F_2$ transition of Eu^{3+} ion, and the defect-related PL (the broad emission ~600 nm) of the Eu-treated ZnO NWs changed with temperature.

is excluded. Therefore, it is believed that the broad visible band emission after Eu^{3+} treatment is purely ascribed to the deep level defect states in ZnO NWs. The physical mechanism of the reduction of DLE will be discussed later. Furthermore, it is noted that there emerges a new peak at ~612 nm, located at the tail of the broad DLE band after Eu^{3+} treatment. This peak is in accordance with the $^5D_0-^7F_2$ transition of the Eu^{3+} ion which usually appears at ~611 nm.

To better understand the optical properties of the Eu-treated ZnO NWs, temperature-dependent PL measurements were performed. As presented in Figure 3a, a series of sharp intense peaks at UV and visible regions can be observed. At low temperatures, the UV emission of the sample is dominated by transition from NBE, such as donor-bound excitons located at 369.5 nm (3.356 eV) and the longitudinal optical (LO) phonon replica of the free excitons (FX). For the visible emission, the

Surface Eu-Treated ZnO NWs

J. Phys. Chem. C, Vol. 114, No. 42, 2010 **18083**
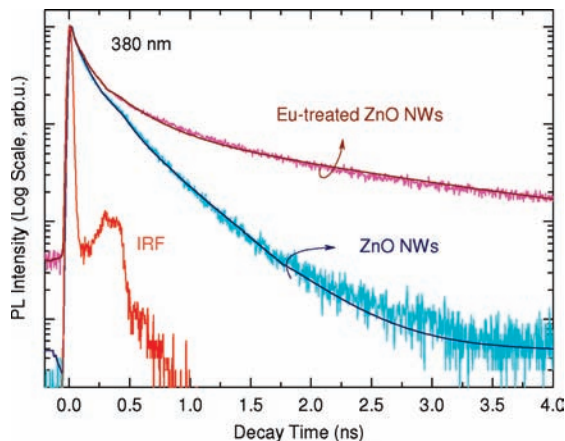
Figure 4. Room temperature TRPL measurement of the ZnO NWs with and without Eu^{3+} treatment.

characteristic bands related to the intra-4f transition of Eu^{3+} ions are clearly observed. It should be mentioned that the excitation wavelength (325 nm) for the PL measurement is within the charge transfer band (CTB) of Eu^{3+} ions, which has very low absorption ability, implying that the emission of Eu^{3+} ions should not be directly excited by the laser but mediated by ZnO. On the other hand, at low temperatures, the intensity of Eu^{3+}-related emission is even higher than the NBE of ZnO NWs, indicating the high probability of energy transfer from ZnO to Eu^{3+} ions. This may open a door to realize the white-light LEDs based on ZnO NWs. Our study provides a proof-of-concept demonstration that ZnO NWs can be efficient hosts for Eu^{3+} emission using this "core/shell" structure.

With the increase of temperature, the intensity of those sharp peaks gradually drops. However, the NBE and the $^5D_0-^7F_2$ transition of the Eu^{3+} ion still exist up to room temperature. Figure 3b−c presents the temperature dependence of the NBE, the $^5D_0-^7F_2$ transition of Eu^{3+} ion, and the defect-related PL intensity (the broad emission ~600 nm) of the Eu-treated ZnO NWs. If the energy transfer from deep level defects to Eu^{3+} ions determines the efficiency of the Eu^{3+}-related PL, it is expected that the intensity change with temperature is similar to that of the defect-related emission, because the Eu^{3+}-related PL intensity is proportional to the number of carriers trapped at the defects of ZnO NWs.[21] However, the temperature dependence of $^5D_0-^7F_2$ transition from Eu^{3+} ion is similar to the NBE of ZnO NWs, and this trend is totally different from the defect emission. Therefore, it is concluded that the energy transfer occurs directly from ZnO to Eu^{3+} ions.

To analyze the carrier dynamics to better understand the energy transfer from ZnO to Eu^{3+} ions, TRPL measurements were carried out. Figure 4 provides the room temperature PL decay kinetics of ZnO NWs with and without Eu^{3+} treatment monitored at 380 nm. The decay curve can be well-described by a biexponential fit with reconvolution,

$$I(t) = \int_{-\infty}^{t} IRF(t') \sum_{i=1}^{2} A_i e^{-t-t'/\tau_i} \, dt' \qquad (1)$$

where A_i is the amplitude of the ith component at time zero, τ_i is the corresponding lifetime, and IRF is the instrument response function. It is found that, from the fitting results, the short lifetime component is ~0.15 ns (80%) which is the same for samples with and without Eu^{3+} treatment. As the long lifetime

component is sensitive to Eu^{3+} treatment, we can focus on this component only for further discussion.

The PL decay time of bare ZnO NWs (τ_{ZnO}) and ZnO NWs with Eu^{3+} ion treatment ($\tau_{ZnO:Eu}$) can be expressed as the following expression, respectively.

$$\frac{1}{\tau_{ZnO}} = \frac{1}{\tau_R} + \frac{1}{\tau_{NR}} \quad \text{and} \quad \frac{1}{\tau_{ZnO:Eu}} = \frac{1}{\tau_R^*} + \frac{1}{\tau_{NR}^*} + \frac{1}{\tau_{ET}}$$
$$(2)$$

where τ_R (τ_R^*) and τ_{NR} (τ_{NR}^*) are the radiative and nonradiative decay times of ZnO NWs. $1/\tau_{ET}$ is the energy transfer rate from ZnO NWs to Eu^{3+} ions. It is expected that the radiative recombination rate should be similar before and after Eu^{3+} ions treatment ($\tau_R \approx \tau_R^*$). If the nonradiative decay time remains unchanged, the decay time of ZnO ($\tau_{ZnO:Eu}$) is expected to be shorter if energy transfer exists due to the addition of channel for carriers. In contrast with expectations, the Eu-treated ZnO NWs display a longer decay time (1.40 ns) than pure ZnO NWs (0.45 ns), indicating the change of nonradiative decay time after post Eu^{3+} ion treatment. The reason can be ascribed to the surface modification of the Eu_2O_3-like layer located at the boundaries of ZnO NWs.[22] In ZnO there exist some intrinsic defects, such as oxygen vacancies. The defects at the surface may act as adsorption sites for O_2 and H_2O. Those sites can trap free electrons and serve as nonradiative recombination centers. This phenomenon is expected to be more significant in NWs due to the larger surface-to-volume ratio. After Eu^{3+} ion treatment, the ZnO NWs are coated with an Eu_2O_3-like layer, which can remarkably decrease the nonradiative recombination rate ($1/\tau_{NR}^* \ll 1/\tau_{NR}$). Thus the PL decay time of Eu-treated ZnO NWs is even longer than that of pure ZnO NWs, although there is an additional decay channel.[23] The interpretation is also consistent with the observations presented in Figure 2 so that, after Eu-treatment, the DLE of ZnO NWs is greatly suppressed.

Generally speaking, direct energy transfer from ZnO to Eu^{3+} ions is difficult to achieve due to the shorter lifetime of exciton in ZnO, the difference of ionic radii, and charges between Eu^{3+} and Zn^{2+} ions. Nevertheless, the Eu_2O_3-like layer not only plays an important role in the surface modification of ZnO NW but also serves as a medium for direct energy transfer from ZnO to Eu^{3+} ions. At the boundaries of ZnO NWs and the Eu_2O_3-like layers, surface shallow level defects may be generated. Taking into account the bandgap of 3.37 eV (368 nm in wavelength) of ZnO, the shallow level may be in line with the $^7F_0-^5L_6$ absorption band of Eu^{3+} ions (393 nm). Those defects located at the boundaries can serve as energy trap centers and support the transfer of energy in the system.[24]

On the basis of the above discussion, we illustrate the tentative excitation and emission processes of the UV-excited Eu^{3+} emission in our sample, and the schematic processes are shown in Figure 5. First, under optical excitation, a large number of carriers are excited from valence band (VB) to conduction band (CB) in ZnO NWs. Then, some of the excited carriers are trapped at the donor level or the interface and consequently recombined, resulting in the DLE (process 2) and NBE (process 3). At the same time, part of the emitted photons of NBE may be reabsorbed by Eu^{3+} ions (process 4). On the other hand, the energy level of carriers trapped at the interface is parallel to the excited states of Eu^{3+} ions, and therefore the energy will resonantly transfer from the shallow level of ZnO to Eu^{3+} ions (process 5). After a fast relaxation, the excited carriers in Eu^{3+} ions radiatively recombine and give rise to the intense $^5D_0-^7F_J$
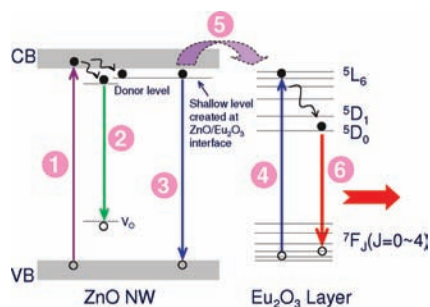
Figure 5. Schematic processes of intense red emission in Eu^{3+} treat ZnO NWs under UV excitation.

red emission. The large ratio of surface to volume in a NW structure should be favorable to the resonant energy transfer.

Conclusions

In conclusion, we have studied the optical properties and energy transfer mechanism of Eu-treated ZnO NWs. The sample exhibits sharp intense red emission related to the intra-4f transition of Eu^{3+} ions. It is found that the Eu^{3+} ions are in the Eu_2O_3-like state located at the surface of ZnO NWs, which play an important role for surface modification of ZnO NWs. Moreover, the Eu_2O_3-like layers serve as efficient energy trap centers supporting the direct energy transfer from ZnO to Eu^{3+} ions.

References and Notes

(1) Sun, H. D.; Makino, T.; Segawa, Y.; Kawasaki, M.; Ohtomo, A.; Tamura, K.; Koinuma, H. *J. Appl. Phys.* **2002**, *91*, 1993.

(2) Tang, Z. K.; Wong, G. K. L.; Yu, P.; Kawasaki, M.; Ohtomo, A.; Koinuma, H.; Segawa, Y. *Appl. Phys. Lett.* **1998**, *72*, 3270.

(3) Sun, H. D.; Segawa, Y.; Kawasaki, M.; Ohtomo, A.; Tamura, K.; Koinuma, H. *J. Appl. Phys.* **2002**, *91*, 6457.

(4) Ryu, Y. R.; Lee, T. S.; Lubguban, J. A.; Corman, A. B.; White, H. W.; Leem, J. H.; Han, M. S.; Park, Y. S.; Youn, C. J.; Kim, W. J. *Appl. Phys. Lett.* **2006**, *88*, 052103.

(5) Sun, H. D.; Makino, T.; Tuan, N. T.; Segawa, Y.; Tang, Z. K.; Wong, G. K. L.; Kawasaki, M.; Ohtomo, A.; Tamura, K.; Koinuma, H. *Appl. Phys. Lett.* **2000**, *77*, 4250.

(6) Makino, T.; Segawa, Y.; Kawasaki, M.; Ohtomo, A.; Shiroki, R.; Tamura, K.; Yasuda, T.; Koinuma, H. *Appl. Phys. Lett.* **2001**, *78*, 1237.

(7) Yang, W. F.; Liu, B.; Chen, R.; Wong, L. M.; Wang, S. J.; Sun, H. D. *Appl. Phys. Lett.* **2010**, *97*, 061911.

(8) Fan, X. F.; Sun, H. D.; Shen, Z. X.; Kuo, J. L.; Lu, Y. M. *J. Phys.: Condens. Matter* **2008**, *20*, 235221.

(9) Wang, K.; Martin, R. W.; O'Donnell, K. P.; Katchkanov, V.; Nogales, E.; Lorenz, K.; Alves, E.; Ruffenach, S.; Briot, O. *Appl. Phys. Lett.* **2005**, *87*, 112107.

(10) Zeng, X.; Yuan, J.; Wang, Z.; Zhang, L. *Adv. Mater.* **2007**, *19*, 4510.

(11) Yang, Y. H.; Feng, Y.; Zhu, H. G.; Yang, G. W. *J. Appl. Phys.* **2010**, *107*, 053502.

(12) Sakaguchi, I.; Sato, Y.; Ryoken, H.; Hishita, S.; Ohashi, N.; Haneda, H. *Jpn. J. Appl. Phys., Part 2* **2005**, *44*, L1289.

(13) Bhargava, R. N.; Chhabra, V.; Som, T.; Ekimov, A.; Taskar, N. *Phys. Status Solidi B* **2002**, *229*, 897.

(14) Chen, L.; Zhang, J. H.; Zhang, X. M.; Liu, F.; Wang, X. J. *Opt. Express* **2008**, *16*, 11795.

(15) Pan, C. J.; Chen, C. W.; Chen, J. Y.; Huang, P. J.; Chi, G. C.; Chang, C. Y.; Ren, F.; Pearton, S. J. *Appl. Surf. Sci.* **2009**, *256*, 187.

(16) Liu, Y.; Luo, W.; Li, R.; Liu, G.; Antonio, M. R.; Chen, X. *J. Phys. Chem. C* **2008**, *112*, 686.

(17) Sun, X. W.; Ling, B.; Zhao, J. L.; Tan, S. T.; Yang, Y.; Shen, Y. Q.; Dong, Z. L.; Li, X. C. *Appl. Phys. Lett.* **2009**, *95*, 133124.

(18) Chen, R.; Xing, G. Z.; Gao, J.; Zhang, Z.; Wu, T.; Sun, H. D. *Appl. Phys. Lett.* **2009**, *95*, 061908.

(19) Huang, W. L.; Labis, J.; Ray, S. C.; Liang, Y. R.; Pao, C. W.; Tsai, H. M.; Du, C. H.; Pong, W. F.; Chiou, J. W.; Tsai, M. H.; Lin, H. J.; Lee, J. F.; Chou, Y. T.; Shen, J. L.; Chen, C. W.; Chi, G. C. *Appl. Phys. Lett.* **2010**, *96*, 062112.

(20) Ahn, C. H.; Kim, Y. Y.; Kim, D. C.; Mohanta, S. K.; Cho, H. K. *J. Appl. Phys.* **2009**, *105*, 013502.

(21) Ishizumi, A.; Kanemitsu, Y. *Appl. Phys. Lett.* **2005**, *86*, 253106.

(22) Liu, K. W.; Chen, R.; Xing, G. Z.; Wu, T.; Sun, H. D. *Appl. Phys. Lett.* **2010**, *96*, 023111.

(23) Liu, K. W.; Tang, Y. D.; Cong, C. X.; Sum, T. C.; Huan, A. C. H.; Shen, Z. X.; Li, W.; Jiang, F. Y.; Sun, X. W.; Sun, H. D. *Appl. Phys. Lett.* **2009**, *94*, 151102.

(24) Fu, Z. P.; Yang, B. F.; Li, L.; Dong, W. W.; Jia, C.; Wu, W. *J. Phys.: Condens. Matter* **2003**, *15*, 2867.